

PDF hosted at the Radboud Repository of the Radboud University Nijmegen

The following full text is a publisher's version.

For additional information about this publication click this link.

<http://hdl.handle.net/2066/175417>

Please be advised that this information was generated on 2019-12-04 and may be subject to change.

Article 25fa pilot End User Agreement

This publication is distributed under the terms of Article 25fa of the Dutch Copyright Act (Auteurswet) with explicit consent by the author. Dutch law entitles the maker of a short scientific work funded either wholly or partially by Dutch public funds to make that work publicly available for no consideration following a reasonable period of time after the work was first published, provided that clear reference is made to the source of the first publication of the work.

This publication is distributed under The Association of Universities in the Netherlands (VSNU) 'Article 25fa implementation' pilot project. In this pilot research outputs of researchers employed by Dutch Universities that comply with the legal requirements of Article 25fa of the Dutch Copyright Act are distributed online and free of cost or other barriers in institutional repositories. Research outputs are distributed six months after their first online publication in the original published version and with proper attribution to the source of the original publication.

You are permitted to download and use the publication for personal purposes. All rights remain with the author(s) and/or copyrights owner(s) of this work. Any use of the publication other than authorised under this licence or copyright law is prohibited.

If you believe that digital publication of certain material infringes any of your rights or (privacy) interests, please let the Library know, stating your reasons. In case of a legitimate complaint, the Library will make the material inaccessible and/or remove it from the website. Please contact the Library through email: copyright@ubn.ru.nl, or send a letter to:

University Library Radboud University
Copyright Information Point PO Box 9100 6500 HA Nijmegen
You will be contacted as soon as possible.

Direct Hyperpolarization of Nitrogen-15 in Aqueous Media with Parahydrogen in Reversible Exchange

Johannes F. P. Colell,[†] Meike Emondts,[‡] Angus W. J. Logan,[†] Kun Shen,[†] Junu Bae,[†] Roman V. Shchepin,[§] Gerardo X. Ortiz, Jr.,[†] Peter Spannring,^{||} Qiu Wang,[†] Steven J. Malcolmson,[†] Eduard Y. Chekmenev,^{§,⊥} Martin C. Feiters,^{||} Floris P. J. T. Rutjes,^{||} Bernhard Blümich,^{*,‡,‡} Thomas Theis,^{*,†,||} and Warren S. Warren^{*,†,‡}

[†]Department of Chemistry, Duke University, Durham, North Carolina 27708, United States

[‡]Institute for Technical and Macromolecular Chemistry, RWTH Aachen University, Worringerweg 2, 52072 Aachen, Germany

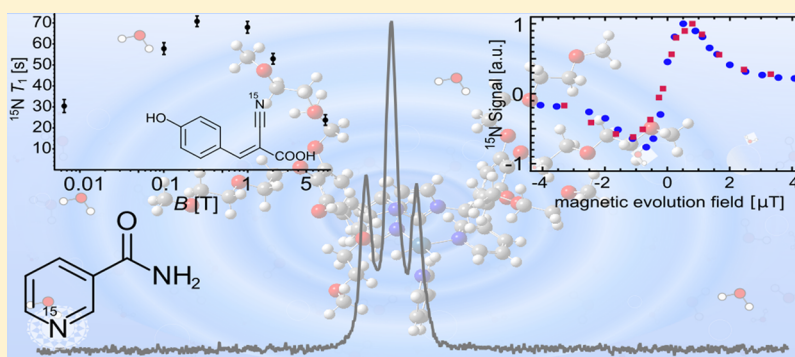
[§]Departments of Radiology and Radiological Sciences, Biomedical Engineering, Physics and Astronomy, Vanderbilt Institute of Imaging Science (VUIIS), Vanderbilt Ingram Cancer Center (VICC), Vanderbilt University, Nashville, Tennessee 37232, United States

^{||}Institute for Molecules and Materials, Radboud University, Heyendaalseweg 135, 6525 AJ Nijmegen, The Netherlands

[⊥]Russian Academy of Sciences, Moscow, Russia

[#]Departments of Physics, Radiology and Biomedical Engineering, Duke University, Durham, North Carolina 27707, United States

S Supporting Information



ABSTRACT: Signal amplification by reversible exchange (SABRE) is an inexpensive, fast, and even continuous hyperpolarization technique that uses *para*-hydrogen as hyperpolarization source. However, current SABRE faces a number of stumbling blocks for translation to biochemical and clinical settings. Difficulties include inefficient polarization in water, relatively short-lived ¹H-polarization, and relatively limited substrate scope. Here we use a water-soluble polarization transfer catalyst to hyperpolarize nitrogen-15 in a variety of molecules with SABRE-SHEATH (SABRE in shield enables alignment transfer to heteronuclei). This strategy works in pure H₂O or D₂O solutions, on substrates that could not be hyperpolarized in traditional ¹H-SABRE experiments, and we record ¹⁵N *T*₁ relaxation times of up to 2 min.

INTRODUCTION

NMR and MRI are nondestructive methods to obtain information about molecular structure and spatial morphology. However, magnetic resonance is restricted mainly by the inherently low sensitivity as a result of low thermal polarization levels. For example, NMR spectroscopy and clinical MRI predominantly use highly abundant ¹H nuclei. Even so, observation of low concentration analytes remains challenging. Hyperpolarization methods (e.g., DNP, PHIP, SABRE, SEOP)^{1–7} enhance MR signals by 4–5 orders of magnitude and overcome inherent sensitivity limitations.^{9–12}

Traditionally, hyperpolarization methods require extensive optimization. Usually methods and optimization are associated with high experimental complexity and cost. In this regard,

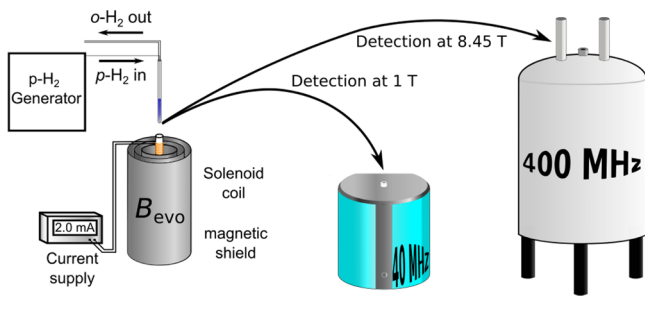
signal amplification by reversible exchange (SABRE) stands out because it is simple, fast, and continuously repeatable.^{4,13} SABRE uses readily available *para*-hydrogen (*p*-H₂) as a source of polarization. The transfer occurs in reversibly formed substrate–hydrogen adducts in a transition metal complex. The magnetic evolution field *B*_{evo} must be sufficiently low to mix energy levels between hydride-¹H and the target nucleus to establish a path for polarization transfer.^{7,14} While protons in the substrate are targeted at magnetic fields around 65 G,¹⁵ transfer to heteronuclei (e.g., ¹⁵N, ¹³C, ³¹P) occurs at μT magnetic fields using a technique termed SABRE in shield

Received: January 17, 2017

Published: April 26, 2017

enables alignment transfer to heteronuclei (SABRE-SHEATH).^{7,8} As shown in Scheme 1, the required hardware is relatively simple.

Scheme 1. A sample is hyperpolarized via SABRE-SHEATH for an evolution time t_{evo} at optimized matching field B_{evo} of ~ 0.5 μT established by a small solenoid coil in a magnetic shield that attenuates the Earth's magnetic field and transferred into a Benchtop (1 T) NMR spectrometer or conventional high-field (8.45 T) spectrometer for detection.



As a result of experimental simplicity and its promise, SABRE and SABRE-SHEATH are now attracting an increasing number of research groups contributing to its rapid development.^{4,7,15–21} A milestone for SABRE was the transition from organic solvents to aqueous solutions, which was recently achieved for ^1H -SABRE.^{22–28}

Still, for ^1H spin–lattice relaxation times are relatively short and the substrate scope is limited. Direct polarization transfer to heteronuclei has not been demonstrated in an aqueous environment. Hyperpolarizing nitrogen-15 via SABRE-SHEATH allows a wider range of structural motifs, and relaxation times are characteristically larger.

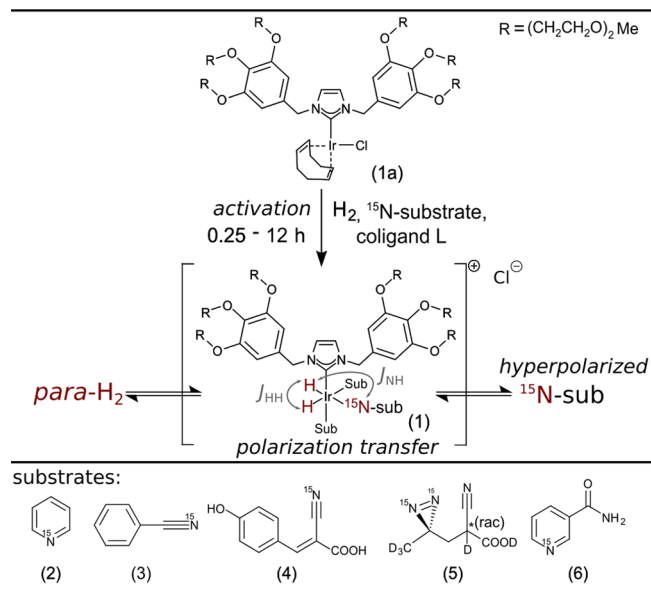
SABRE-SHEATH with ^{15}N targets is made accessible with the water-soluble $[\text{IrCl}(\text{IDEg})(\text{COD})]$ precatalyst (**1a**). As shown in Scheme 2 the precatalyst is converted to the catalytically active species (**1**) in the presence of substrates under a hydrogen atmosphere.²² At μT magnetic field hydride and ^{15}N energy levels match and the spin system coherently evolves with a rate given by J_{NH} into ^{15}N -polarization on substrates.²⁹

We investigate different molecular motifs found in medical drugs, biomolecules, and molecular tags. Structural motifs could be readily translated from the established $[\text{IrCl}(\text{IMes})(\text{COD})]$ system.^{16,30}

Pyridine (**2**), the canonical SABRE substrate,⁴ was a logical first choice. Next, nitriles are often encountered in drugs,³¹ polarize consistently well, tolerate complex backbones, and show large ^{15}N -SABRE-SHEATH enhancements, despite little to no ^1H -SABRE enhancements.^{30,32} We selected benzonitrile (**3**) and α -cyano-4-hydroxycinnamic acid (**4**) (CHCA, buffered with NaOD to pH 7.5). Diazirines, which also do not exhibit ^1H enhancements, are common biomolecular tags that can replace CH_2 groups in many classes of biomolecules.³³ Here we use 2-cyano-3-(D_3 -methyl- $^{15}\text{N}_2$ -diazirine)propanoic acid (**5**). Lastly, we focus on nicotinamide (**6**), the amide of vitamin B_3 , which could be tolerated in vivo at detectable concentrations^{34–36} and is a potential option for translation to biomedical studies.^{20,37}

For these substrates we detail hyperpolarization levels, carefully characterize temperature and magnetic field dependencies, consider the effect of deuterated vs protonated solvents

Scheme 2. Precatalyst $[\text{IrCl}(\text{IDEg})(\text{COD})]$ (**1a**) is transformed into the active species $[\text{Ir}(\text{IDEg})(\text{H})_2\text{Sub}_3]$ (**1**) in presence of a substrate of choice (**2–6**) under a hydrogen atmosphere; reversible exchange leads to polarization buildup on ^{15}N within 30–120 s; the polarization transfer is primarily driven by the N–H coupling through the bonds that form a 180° angle as the N–H coupling through bonds forming a 90° angle is close to zero.



(D_2O vs H_2O), and measure relaxation time constants at various magnetic fields.

RESULTS AND DISCUSSION

In Figure 1 we show a comparison between single-scan spectra originating from compounds directly SABRE-SHEATH hyperpolarized in aqueous medium, referenced to thermally polarized neat ^{15}N -pyridine at 8.45 T. Concentrations of investigated compounds are different as a result of solubility as well as sample loss phenomena for benzonitrile and pyridine. Both pyridine and benzonitrile were initially prepared as 100 mM solutions, but after activation by H_2 bubbling the concentrations were significantly reduced.

A synopsis of experimental results and conditions is given in Table 1 (experimental details provided in Materials and Methods). Spectra are acquired at 1 T and 8.45 T (see Scheme 1) to study the field dependence of T_1 relaxation as detailed below. The 1 T measurements also demonstrate the feasibility of high-sensitivity single-scan ^{15}N detection with a benchtop NMR system. Furthermore, to determine the effect of proton-containing solvents, nicotinamide was investigated in H_2O .

We find that polarization levels in deuterated solvents are largely independent of the detection field; that is, enhancements simply scale with the thermal polarization. In contrast, for nicotinamide in H_2O (Table 1, entry 6), we observe lower apparent polarization levels at 8.45 T. This is caused by relaxation losses during transfer because it takes much longer to transfer the sample into the high-field magnet (~ 8 s) than into the benchtop device sitting right next to the magnetic shields (~ 2 s). The solvent protons (and deuterons) are in chemical exchange with the ^{15}N -substrate, where they cause spin–dipole

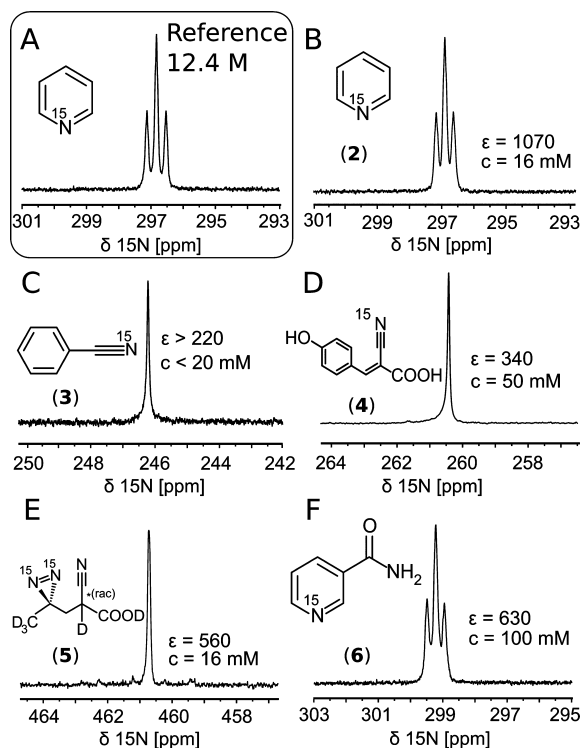


Figure 1. ^{15}N spectra of (A) thermally polarized reference at 8.45 T and (B–F) hyperpolarized compounds (in D_2O unless denoted otherwise). (A) Neat ^{15}N -pyridine, (B) ^{15}N -pyridine, (C) ^{15}N -benzonitrile, (D) ^{15}N -CHCA, (E) $^{15}\text{N}_2$ -diazirine, (F) ^{15}N -nicotinamide (in H_2O).

relaxation. This relaxation mechanism scales with the distance between the relaxation partners r_{ij}^{-6} as well as the gyromagnetic ratio, which is 6.5 times smaller for deuterium,^{38,39} explaining the observed differences between solvents.

SABRE-SHEATH in water gives rise to a new set of challenges. Water has significantly higher viscosity and surface tension than methanol, and at room temperature the solubility of hydrogen in water is 5 times lower.^{40,41} We observed that some samples, specifically nonpolar liquid-state substrates (e.g., benzonitrile and pyridine), are extracted from the solvent when bubbling with hydrogen during the polarization buildup. Nicotinamide and CHCA, both crystalline solids when isolated, were used for systematic studies, as substrate loss did not occur.²⁰

Of particular interest are the dependence of the ^{15}N polarization on temperature and magnetic evolution field B_{evo} . Figure 2 contrasts the established $[\text{IrCl}(\text{IMes})(\text{COD})]$ in

methanol and catalyst **1** in $\text{H}_2\text{O}/\text{D}_2\text{O}$ as a function of these variables (T , B_{evo}).

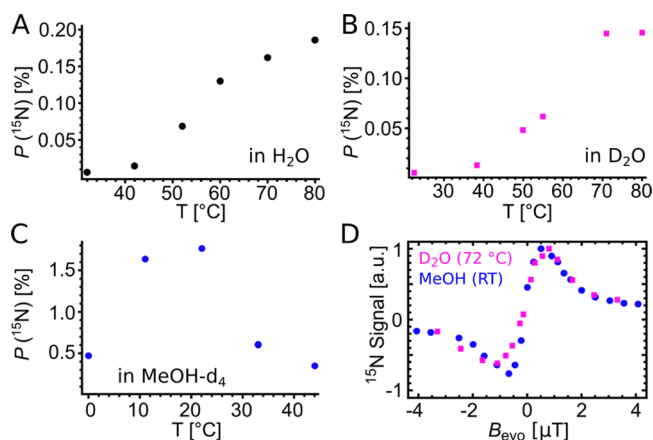


Figure 2. Comparison of ^{15}N polarization as a function of temperature in (A) H_2O , (B) D_2O , and (C) methanol- d_4 at $B_{\text{evo}} = 0.5 \mu\text{T}$. (D) Hyperpolarized signals as a function of μT field at the temperature corresponding to the maximum polarization in the respective solvents: 22 °C for ^{15}N -acetonitrile in methanol- d_4 and 72 °C for ^{15}N -CHCA in D_2O (blue: 5 mM $[\text{IrCl}(\text{IMes})(\text{COD})]$, 30 mM pyridine, 100 mM ^{15}N - CH_3CN , methanol- d_4 ; magenta: 5 mM $[\text{IrCl}(\text{IDEG})(\text{COD})]$, 30 mM pyridine, 50 mM ^{15}N -CHCA, D_2O).

The temperature dependence was studied using a 100 mM nicotinamide sample. For catalyst system **1** in H_2O (Figure 2A) and D_2O (Figure 2B) the ^{15}N polarization increases with temperature. In contrast, in methanol (Figure 2C, $[\text{IrCl}(\text{IMes})(\text{COD})]$ precursor) the largest polarization is recorded at room temperature.

The magnetic field dependence is shown in Figure 2D. We compare normalized data (max. ^{15}N polarization: 0.13% in D_2O , 1.7% in $\text{MeOH}-d_4$) of two nitrile/solvent systems: first, in blue, ^{15}N -acetonitrile in $\text{MeOH}-d_4$ with $[\text{IrCl}(\text{IMes})(\text{COD})]$ and second, in magenta, ^{15}N -CHCA in D_2O with $[\text{IrCl}(\text{IDEG})(\text{COD})]$ (**1a**).

We note that nitriles are better suited for this study than nicotinamide, as enhancements are more robust and reproducible. Additionally, they exhibit inversion of the NMR signal upon inversion of B_{evo} . Variation of the temperature changes the dissociation rate constants of substrate and catalyst-bound H_2 .^{14,16,42} Optimal polarization transfer efficiency is expected when the exchange rate k_{diss} is on the order of the ^{15}N to hydride J_{NH} -coupling across the iridium center (see Scheme 2).^{14,42} Figure 1A–C show that the IMes catalyst in methanol yields the largest ^{15}N polarization at room temperature,

Table 1. Synopsis of Experimental Conditions, Enhancements, and Polarization Levels^a

substrate	activation time [h]	$c_{\text{substrate}}/c_{\text{catalyst}}$	$c_{\text{substrate}}$ [mM]	enhancement 8.45 T (P [%])	enhancement 1 T (P [%])	enhancement ratio (1 T/8.45 T)
(2) pyridine	12	3.3	16.5 ^c	1100	^d	^d
(3) benzonitrile	0.25	20	50 ^{b,c}	90	^d	^d
(4) CHCA	12	10	50	440 (0.13)	3700 (0.13)	8.4
(5) diazirine	6	10	16.3	560 (0.16)	4700 (0.17)	8.4
(6) nicotinamide	12	20	100	520 (0.16)	6100 (0.21)	8.9
(6) nicotinamide H_2O	12	20	100	630 (0.2)	10 500 (0.37)	28

^aSubstrates are ^{15}N labeled, solvent is D_2O unless otherwise specified. Concentrations of liquid substrates are determined at the time of the experiment using ^1H spectroscopy. $T = 75 \text{ }^\circ\text{C}$. ^bSignal maximum obtained 30 min after activation, subsequent substrate loss due to evaporation.

^cInitial concentration 100 mM. ^dInsufficient S/N ratio.

whereas catalyst **1** requires significantly elevated temperatures to achieve comparable exchange rates leading to maximum polarization. On the basis of these insights it is reasonable to expect ^{15}N polarization in water to decrease at even higher temperatures, in analogy to methanol, as shown in Figure 2C.

As seen in Figure 2D, the methanol and water systems show very similar responses to B_{evo} at their respective optimized temperatures (22 and 72 °C). The response curves originate from two distinct matching conditions associated with overpopulation in $^{15}\text{N}-\alpha$ or $^{15}\text{N}-\beta$, giving either positive or negative NMR signal with identical polarization levels.³⁰ The matching conditions are given by⁷

$$B_{\text{evo}} = \pm \frac{J_{\text{HH}} + J_{\text{NH}}/2}{\gamma_{\text{H}} - \gamma_{\text{N}}} \quad (1)$$

where J_{HH} is the hydride to hydride J -coupling (~ 10 Hz) and J_{NH} the hydride to ^{15}N coupling (~ 20 Hz) in **1**. Experimentally, we observe maxima at $B_{\text{evo}} \approx \pm 0.5$ μT , which is slightly higher than the ± 0.3 μT predicted from eq 1, as the limited lifetime broadens the matching conditions.

Taken together, the observations of Figure 1A–D suggest that the activation energy of substrate dissociation from **1** is significantly larger than for the established $[\text{IrCl}(\text{IMes})-(\text{COD})]$ –methanol systems. This is also supported by the fact that catalyst **1** in methanol at RT did not yield any enhancement.

The absolute polarization level in D_2O is about one order of magnitude smaller than for the methanol system, when compared at their respective optimized temperatures (^{15}N -CHCA in D_2O , $P(^{15}\text{N}) = 0.13\%$, ^{15}N - CH_3CN in d_4 -MeOH, $P(^{15}\text{N}) = 1.7\%$). Interestingly, this difference in hyperpolarization level can simply be attributed to the difference in hydrogen solubility (factor 5) and the difference in solvent concentration ($c(\text{H}_2\text{O}) = 55$ mol/L, $c(\text{MeOH}) = 28$ mol/L, factor 2).

Current experimental data and theoretical considerations indicate that SABRE polarization levels are limited by the exchange of hydrides on the iridium center and the exchange kinetics of other ligand types (substrate/solvent), as well as both pressure and flow rate of *para*-hydrogen. Exchange of hydrogen restores the polarization source to the active complex species and the process proceeds via the mixed classical/nonclassical hydride $[\text{Ir}(\text{H})_2(\eta\text{-H}_2)(\text{IMes})\text{L}_2]$, with arbitrary ligands L .^{14,16} Formation of this species requires collision between a 16-electron complex and a hydrogen molecule, where collision with a *para*-hydrogen molecule may refresh the active species. As a result, the polarization is proportional to the concentration of *para*-hydrogen in solution, not the saturation concentration of hydrogen (*ortho* + *para*). Accordingly, the pressure dependence of polarizations is relatively weak, whereas dependence on the flow rate is significant. Depending on system composition, a linear or exponential dependence of ^{15}N polarization on the flow rate was reported.^{30,43,44} We conclude that the *para*-hydrogen enrichment in solution is limited by the exchange at the gas–liquid interface.

Let us now consider the substrate exchange process. The rates of ligand dissociation k_{diss} and association k_{asso} determine not only the lifetime of the complex, where polarization transfer from the hydrides to the target nuclei occurs, but also the concentration of the 16-electron species required for the hydride exchange.¹⁴ As a result ^{15}N polarization depends directly on the concentration of the 16-electron species.

Accordingly, the largest polarizations are observed at relatively low catalyst concentrations and high catalyst loadings. It is noteworthy that an exponential dependence of polarization on the substrate concentrations has been observed by Appleby et al.⁴⁵

We point out that all reported polarization levels are not optimized with respect to sample composition, concentrations, hydrogen pressure, or flow rate. Optimization of catalyst concentration and loading afforded an 8–10-fold increase of ^{15}N polarization level for the methanol system. Maximum polarizations are recorded at low catalyst concentrations and high catalyst loadings (^{15}N -nicotinamide $P(^{15}\text{N}) = 7\%$, ^{15}N -benzonitrile $P(^{15}\text{N}) = 16\%$, metronidazole at natural abundance $P(^{15}\text{N}) = 20\%$).^{7,14,18,43,46} We conclude that ^{15}N polarization can be increased by at least a factor 10 by using low substrate concentrations and high catalyst loading. Further improvements are expected by modifications to the experimental setup to allow for more effective mixing of hydrogen and solvent at higher pressures.

^{15}N Relaxation Times in Water. Of particular importance for hyperpolarization applications is the spin–lattice relaxation time T_1 , which defines the viable time delay between preparation of hyperpolarization and detection. We examined the T_1 lifetime for ^{15}N -nicotinamide⁴⁶ and ^{15}N -CHCA, which constitute biocompatible compounds and contain ^{15}N in chemically different environments.^{46–48} Table 2 shows the ^{15}N T_1 relaxation times in D_2O , which at 1 T exceed 1 min for both compounds.

Table 2. ^{15}N T_1 Times of 100 mM Nicotinamide and 50 mM CHCA in D_2O at Different Detection Fields

	T_1 [s] 1 T	T_1 [s] 8.45 T
^{15}N -CHCA	71 ± 15^a	24 ± 3
^{15}N -nicotinamide	116 ± 10	$32^b \pm 4$

^aDetected and stored at 1 T. Control by detection at 8.45 T: $T_1 = 68 \pm 2$ s. ^bIn H_2O : 32 ± 5.5 s.

For ^{15}N -nicotinamide at 8.45 T we find the effect of proton-containing solvent (H_2O) on the T_1 time to be negligible. It should be noted that the ^{15}N T_1 time of nicotinamide at 8.45 T and room temperature is close to the T_1 reported for ^{13}C in the $^{13}\text{C}(1)$ -pyruvate markers currently in clinical use for prostate cancer diagnostics ($T_1 = 29.2$ s in vivo, $T_1 = 60$ s, ex vivo, 3 T).^{9,10} It is noteworthy that the ^{13}C T_1 values in vivo are smaller than those ex vivo, characteristic for diffusion in constricted environments.

To elucidate this field dependence in more detail, we hyperpolarized ^{15}N -CHCA and held the sample at different fields for variable times prior to detection. The results are shown in Figure 3, displaying ^{15}N -relaxation time of CHCA (50 mM, pH 7.5, D_2O) at different magnetic fields. For this compound relatively low magnetic fields of about 0.2 T give the longest relaxation times. This is an intriguing finding in the context of low-field approaches to NMR and MRI,^{49,50} which could be coupled with SABRE to establish low-cost spectroscopy and molecular imaging.

The scaling of signal-to-noise with magnetic field strongly depends on the exact experimental conditions. For traditional thermal NMR, the signal is proportional to polarization and the induction. Both terms are proportional to B_0 ; thus the signal scales with B_0^2 .^{38,51} In NMR, coil noise is typically dominant,

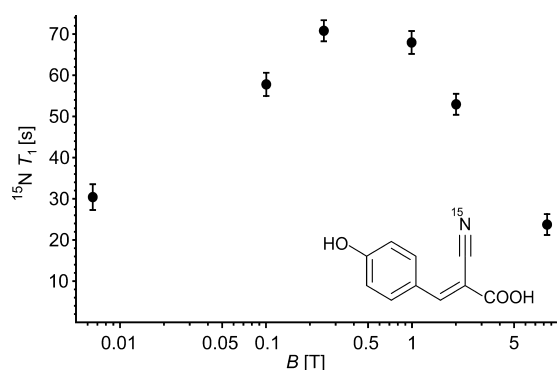


Figure 3. ^{15}N T_1 time constant of CHCA as a function of the magnetic field. The sample is hyperpolarized and stored at a given field for an incremented delay time and detected at 8.45 T.

which scales as $B_0^{1/4}$; hence signal-to-noise (S/N) is proportional to $B_0^{7/4}$.^{51–53} However, with a hyperpolarized sample spin polarization is independent of B_0 and, thus, S/N scales with $B_0^{3/4}$.

Another scenario arises for human MRI. Here, dielectric losses dominate, which are proportional to B_0 . Thus, S/N only increases proportional to B_0 for thermal MRI experiments.^{52,54} Therefore, S/N is expected to be independent of B_0 for hyperpolarized human MRI.^{55,56} MRI in low magnetic fields has significant advantages, as magnet and RF-circuit design are flexible, easy to construct, and relatively inexpensive.^{56,57} For example, high-performance ^1H -MRI at 6.5 mT with thermal magnetization has already been reported.⁴⁹ It is noteworthy that recent advances in the low-field domain, such as “external high-quality-factor-enhanced NMR” (EHQE-NMR)⁵⁸ and others,⁵⁹ lead to S/N independent of B_0 even for spectroscopic applications.

MATERIALS AND METHODS

Solutions of substrates in $\text{D}_2\text{O}/\text{H}_2\text{O}$ were added to $[\text{IrCl}(\text{IDEG})-(\text{COD})]$ (IDEG = 1,3-bis(3,4,5-tris(diethyleneglycol)benzyl)-imidazole-2-ylidene), COD = 1,5-cyclooctadiene), stirred until a homogeneous solution of known concentration in catalyst is obtained, and transferred to a 5 mm medium wall pressure NMR tube (Wilmad 524-PV-7). The typical sample volume was 350 μL . The solution was bubbled with argon for 30 min and pressurized with 10 bar of *para*- H_2 , and hydrogen flow was adjusted to obtain adequate bubbling. Catalyst activation times were 0.25–12 h depending on substrate, solvent (deuterated solvents require longer activation times), and temperature. Catalyst activation can be sped up significantly by raising the temperature. For SABRE-SHEATH experiments *para*- H_2 (Bruker BPHG 090, 38 K, 90%) was bubbled through a sample placed in a μT magnetic field. Hyperpolarization buildup is achieved in 0.5–2 min. The μT field is generated by a small solenoid inside a magnetic shield (see Scheme 1). The sample temperature was controlled with a water bath inside the magnetic shields. Measurements were performed with a Bruker Avance DX 360 (8.45 T) or Magritek Spinsolve $^1\text{H}/^{15}\text{N}$ spectrometer (1 T). Enhancements are calculated relative to neat ^{15}N -labeled pyridine. The concentration in the samples was monitored by ^1H spectroscopy.

CONCLUSIONS

We have demonstrated SABRE-SHEATH hyperpolarization of ^{15}N in aqueous media at moderate temperatures (20–80 $^\circ\text{C}$) and achieve up to 1000-fold enhancements over thermal measurements at 8.45 T. We applied SABRE-SHEATH in water to biocompatible marker groups in different molecules (CHCA, nicotinamide, diazirine moieties). Hyperpolarization

of ^{15}N -nitrile and the $^{15}\text{N}_2$ -diazirine exemplifies how SABRE-SHEATH is amenable to more substrate classes because ^{15}N is closer to the hyperpolarization source than protons in the molecular backbone.

Furthermore, we demonstrated T_1 times comparable to, or exceeding, clinically used DNP tracers.^{9,10} For example, nicotinamide in D_2O exhibits a ^{15}N relaxation time of 2 min, which is significantly longer than typical ^1H - T_1 (seconds) of traditional ^1H -SABRE substrates. Still, recent advances have demonstrated long-lived ^1H singlet states with decay times of up to 4.5 min.³⁷ When such strategies are translated to ^{15}N , lifetimes in excess of 20 min become available.⁶⁰

Imaging applications of SABRE hyperpolarized protons²⁵ as well as nitrogen-15 have already been reported.⁴³ Hyperpolarized heteronuclei are beneficial, as they are background free and have a large chemical shift range, which allows for easy chemical identification. Future developments may be expected to advance SABRE to in vivo molecular imaging complementing DNP-hyperpolarized ^{13}C tracers, which have quickly become an essential and routine tool, giving detailed and fundamental insight into in vivo metabolism and biochemistry.^{9,10,61–65}

ASSOCIATED CONTENT

Supporting Information

The Supporting Information is available free of charge on the ACS Publications website at DOI: 10.1021/jacs.7b00569.

Relaxation time measurements, detailed description of experimental procedures, spectral data, physicochemical reference data for H_2O (PDF)

AUTHOR INFORMATION

Corresponding Authors

*bluemich@itmc.rwth-aachen.de

*thomas.theis@duke.edu

*warren.warren@duke.edu

ORCID

Johannes F. P. Colell: 0000-0001-9020-344X

Qiu Wang: 0000-0002-6803-9556

Steven J. Malcolmson: 0000-0003-3229-0949

Eduard Y. Chekmenev: 0000-0002-8745-8801

Floris P. J. T. Rutjes: 0000-0003-1538-3852

Thomas Theis: 0000-0001-6779-9978

Notes

The authors declare no competing financial interest.

ACKNOWLEDGMENTS

The authors gratefully acknowledge the NSF (CHE-1363008 and CHE-1416268), NIH 1R21EB018014, P41 EB015897 and 1R21EB020323, DOD CDMRP W81XWH-15-1-0271 and W81XWH-12-1-0159/BC112431, and Duke University for financial support of this research. This work has been supported by Deutsche Forschungsgemeinschaft (DFG-BL231/47-1), as well as by the European Union and the provinces of Gelderland and Overijssel (NL) through the EFRO Ultrasense NMR project. The authors gratefully acknowledge Magritek for supply of the 1 T ^{15}N -spectrometer and friendly technical assistance.

REFERENCES

- (1) Carver, T. R.; Slichter, C. P. *Phys. Rev.* **1956**, *102*, 975–980.

- (2) Cudalbu, C.; Comment, A.; Kurdzesau, F.; van Heeswijk, R. B.; Uffmann, K.; Jannin, S.; Denisov, V.; Kirik, D.; Gruetter, R. *Phys. Chem. Chem. Phys.* **2010**, *12*, 5818–5823.
- (3) Shchepin, R. V.; Coffey, A. M.; Waddell, K. W.; Chekmenev, E. Y. *Anal. Chem.* **2014**, *86*, 5601–5605.
- (4) Adams, R. W.; Aguilar, J. A.; Atkinson, K. D.; Cowley, M. J.; Elliott, P. I. P.; Duckett, S. B.; Green, G. G. R.; Khazal, I. G.; Lopez-Serrano, J.; Williamson, D. C. *Science* **2009**, *323*, 1708–1711.
- (5) Bowers, C. R.; Weitekamp, D. P. *Phys. Rev. Lett.* **1986**, *57*, 2645–2648.
- (6) Ben-Amar Baranga, A.; Appelt, S.; Romalis, M. V.; Erickson, C. J.; Young, A. R.; Cates, G. D.; Happer, W. *Phys. Rev. Lett.* **1998**, *80*, 2801–2804.
- (7) Theis, T.; Truong, M. L.; Coffey, A. M.; Shchepin, R. V.; Waddell, K. W.; Shi, F.; Goodson, B. M.; Warren, W. S.; Chekmenev, E. Y. *J. Am. Chem. Soc.* **2015**, *137*, 1404–1407.
- (8) Barskiy, D. A.; Shchepin, R. V.; Tanner, C.; Colell, J. F. P.; Goodson, B. M.; Theis, T.; Warren, W. S.; Chekmenev, E. Y. *ChemPhysChem* **2017**, DOI: 10.1002/cphc.201700416.
- (9) Kurhanewicz, J.; Vigneron, D. B.; Brindle, K.; Chekmenev, E. Y.; Comment, A.; Cunningham, C. H.; DeBerardinis, R. J.; Green, G. G.; Leach, M. O.; Rajan, S. S.; Rizzi, R. R.; Ross, B. D.; Warren, W. S.; Malloy, C. R. *Neoplasia* **2011**, *13*, 81–97.
- (10) Nelson, S. J.; Kurhanewicz, J.; Vigneron, D. B.; Larson, P. E. Z.; Harzstark, A. L.; Ferrone, M.; van Criekinge, M.; Chang, J. W.; Bok, R.; Park, I.; Reed, G.; Carvajal, L.; Small, E. J.; Munster, P.; Weinberg, V. K.; Ardenkjaer-Larsen, J. H.; Chen, A. P.; Hurd, R. E.; Odegardstuen, L. I.; Robb, F. J.; Tropp, J.; Murray, J. A. *Sci. Transl. Med.* **2013**, *5*, 198ra108–198ra108.
- (11) Eshuis, N.; van Weerdenburg, B. J. A.; Feiters, M. C.; Rutjes, F. P. J. T.; Wijmenga, S. S.; Tessari, M. *Angew. Chem., Int. Ed.* **2015**, *54*, 1372–1372.
- (12) Eshuis, N.; Hermkens, N.; van Weerdenburg, B. J. A.; Feiters, M. C.; Rutjes, F. P. J. T.; Wijmenga, S. S.; Tessari, M. *J. Am. Chem. Soc.* **2014**, *136*, 2695–2698.
- (13) Hövener, J.-B.; Schwaderlapp, N.; Lickert, T.; Duckett, S. B.; Mewis, R. E.; Highton, L. A. R.; Kenny, S. M.; Green, G. G. R.; Leibfritz, D.; Korvink, J. G.; Hennig, J.; von Elverfeldt, D. *Nat. Commun.* **2013**, *4*, 2946.
- (14) Barskiy, D. A.; Pravdivtsev, A. N.; Ivanov, K. L.; Kovtunov, K. V.; Koptuyug, I. V. *Phys. Chem. Chem. Phys.* **2015**, *18*, 89–93.
- (15) Zeng, H.; Xu, J.; Gillen, J.; McMahon, M. T.; Artemov, D.; Tyburn, J.-M.; Lohman, J. A. B.; Mewis, R. E.; Atkinson, K. D.; Green, G. G. R.; Duckett, S. B.; van Zijl, P. C. M. *J. Magn. Reson.* **2013**, *237*, 73–78.
- (16) Cowley, M. J.; Adams, R. W.; Atkinson, K. D.; Cockett, M. C. R.; Duckett, S. B.; Green, G. G. R.; Lohman, J. A. B.; Kerssebaum, R.; Kilgour, D.; Mewis, R. E. *J. Am. Chem. Soc.* **2011**, *133*, 6134–6137.
- (17) Theis, T.; Truong, M.; Coffey, A. M.; Chekmenev, E. Y.; Warren, W. S. *J. Magn. Reson.* **2014**, *248*, 23–26.
- (18) Barskiy, D. A.; Shchepin, R. V.; Coffey, A. M.; Theis, T.; Warren, W. S.; Goodson, B. M.; Chekmenev, E. Y. *J. Am. Chem. Soc.* **2016**, *138*, 8080–8083.
- (19) Nikolaou, P.; Goodson, B. M.; Chekmenev, E. Y. *Chem. - Eur. J.* **2015**, *21*, 3156–3166.
- (20) Shchepin, R. V.; Barskiy, D. A.; Coffey, A. M.; Theis, T.; Shi, F.; Warren, W. S.; Goodson, B. M.; Chekmenev, E. Y. *ACS Sensors* **2016**, *1*, 640–644.
- (21) Shchepin, R. V.; Chekmenev, E. Y. *J. Labelled Compd. Radiopharm.* **2014**, *57*, 621–624.
- (22) Spannring, P.; Reile, I.; Emondts, M.; Schleker, P. P. M.; Hermkens, N. K. J.; van der Zwaluw, N. G. J.; van Weerdenburg, B. J. A.; Tinnemans, P.; Tessari, M.; Blümich, B.; Rutjes, F. P. J. T.; Feiters, M. C. *Chem. - Eur. J.* **2016**, *22*, 9277–9282.
- (23) Truong, M. L.; Shi, F.; He, P.; Yuan, B.; Plunkett, K. N.; Coffey, A. M.; Shchepin, R. V.; Barskiy, D. A.; Kovtunov, K. V.; Koptuyug, I. V.; Waddell, K. W.; Goodson, B. M.; Chekmenev, E. Y. *J. Phys. Chem. B* **2014**, *18*, 13882–13889.
- (24) Fekete, M.; Bayfield, O.; Duckett, S. B.; Hart, S.; Mewis, R. E.; Pridmore, N.; Rayner, P. J.; Whitwood, A. *Inorg. Chem.* **2013**, *52*, 13453–13461.
- (25) Rovedo, P.; Knecht, S.; Bäumlisberger, T.; Cremer, A. L.; Duckett, S. B.; Mewis, R. E.; Green, G. G. R.; Burns, M. J.; Rayner, P. J.; Leibfritz, D.; Korvink, J. G.; Hennig, J.; Pütz, G.; von Elverfeldt, D.; Hövener, J.-B. *J. Phys. Chem. B* **2016**, *120*, 5670–5677.
- (26) Hövener, J.-B.; Schwaderlapp, N.; Borowiak, R.; Lickert, T.; Duckett, S. B.; Mewis, R. E.; Adams, R. W.; Burns, M. J.; Highton, L. A. R.; Green, G. G. R.; Olaru, A.; Hennig, J.; von Elverfeldt, D. *Anal. Chem.* **2014**, *86*, 1767–1774.
- (27) Zeng, H.; Xu, J.; McMahon, M. T.; Lohman, J. A. B.; van Zijl, P. C. M. *J. Magn. Reson.* **2014**, *246*, 119–121.
- (28) Shi, F.; He, P.; Best, Q. A.; Groome, K.; Truong, M. L.; Coffey, A. M.; Zimay, G.; Shchepin, R. V.; Waddell, K. W.; Chekmenev, E. Y.; Goodson, B. M. *J. Phys. Chem. C* **2016**, *120*, 12149–12156.
- (29) Barskiy, D. A.; Pravdivtsev, A. N.; Ivanov, K. L.; Kovtunov, K. V.; Koptuyug, I. V. *Phys. Chem. Chem. Phys.* **2015**, *18*, 89–93.
- (30) Colell, J. F. P.; Logan, A. W. J.; Zhou, Z.; Shchepin, R. V.; Barskiy, D. A.; Ortiz, G. X.; Wang, Q.; Malcolmson, S. J.; Chekmenev, E. Y.; Warren, W. S.; Theis, T. *J. Phys. Chem. C* **2017**, *121*, 6626.
- (31) Fleming, F. F.; Yao, L.; Ravikumar, P. C.; Funk, L.; Shook, B. C. *J. Med. Chem.* **2010**, *53*, 7902–7917.
- (32) Mewis, R. E.; Green, R. A.; Cockett, M. C. R.; Cowley, M. J.; Duckett, S. B.; Green, G. G. R.; John, R. O.; Rayner, P. J.; Williamson, D. C. *J. Phys. Chem. B* **2015**, *119*, 1416–1424.
- (33) Dubinsky, L.; Krom, B. P.; Meijler, M. M. *Bioorg. Med. Chem.* **2012**, *20*, 554–570.
- (34) Bergmann, F.; Wislicki, L. *Br. J. Pharmacol. Chemother.* **1953**, *8*, 49–53.
- (35) Guyton, J. R.; Blazing, M. A.; Hagar, J.; Kashyap, M. L.; Knopp, R. H.; McKenney, J. M.; Nash, D. T.; Nash, S. D. *Arch. Intern. Med.* **2000**, *160*, 1177–1184.
- (36) Libri, V.; Yandim, C.; Athanasopoulos, S.; Loyse, N.; Natisvili, T.; Law, P. P.; Chan, P. K.; Mohammad, T.; Mauri, M.; Tam, K. T.; Leiper, J.; Piper, S.; Ramesh, A.; Parkinson, M. H.; Huson, L.; Giunti, P.; Festenstein, R. *Lancet* **2014**, *384*, 504–513.
- (37) Roy, S. S.; Norcott, P.; Rayner, P. J.; Green, G. G. R.; Duckett, S. B. *Angew. Chem., Int. Ed.* **2016**, *55*, 15642–15645.
- (38) Abragam, A. *The Principles of Nuclear Magnetism*; Clarendon Press: Oxford, 1961.
- (39) Halbach, K. *Nucl. Instrum. Methods* **1980**, *169*, 1–10.
- (40) Crozier, T. E.; Yamamoto, S. *J. Chem. Eng. Data* **1974**, *19*, 242–244.
- (41) Brunner, E. *J. Chem. Eng. Data* **1985**, *30*, 269–273.
- (42) Knecht, S.; Pravdivtsev, A. N.; Hövener, J.-B.; Yurkovskaya, A. V.; Ivanov, K. L. *RSC Adv.* **2016**, *6*, 24470–24477.
- (43) Truong, M. L.; Theis, T.; Coffey, A. M.; Shchepin, R. V.; Waddell, K. W.; Shi, F.; Goodson, B. M.; Warren, W. S.; Chekmenev, E. Y. *J. Phys. Chem. C* **2015**, *119*, 8786–8797.
- (44) Shchepin, R. V.; Truong, M. L.; Theis, T.; Coffey, A. M.; Shi, F.; Waddell, K. W.; Warren, W. S.; Goodson, B. M.; Chekmenev, E. Y. *J. Phys. Chem. Lett.* **2015**, *6*, 1961–1967.
- (45) Appleby, K. M.; Mewis, R. E.; Olaru, A. M.; Green, G. G. R.; Fairlamb, I. J. S.; Duckett, S. B. *Chem. Sci.* **2015**, *6*, 3981–3993.
- (46) Shchepin, R. V.; Barskiy, D. A.; Mikhaylov, D. M.; Chekmenev, E. Y. *Bioconjugate Chem.* **2016**, *27*, 878–882.
- (47) Wang, H.; Lanks, K. W. *Cancer Res.* **1986**, *46*, 5349–5352.
- (48) Olaru, A. M.; Burns, M. J.; Green, G. G. R.; Duckett, S. B. *Chem. Sci.* **2016**, *8*, 2257–2266.
- (49) Saracanie, M.; LaPierre, C. D.; Salameh, N.; Waddington, D. E. J.; Witzel, T.; Rosen, M. S. *Sci. Rep.* **2015**, *5*, 15177.
- (50) Danieli, E.; Mauler, J.; Perlo, J.; Blümich, B.; Casanova, F. J. *Magn. Reson.* **2009**, *198*, 80–87.
- (51) Hoult, D. I.; Richards, R. E. *J. Magn. Reson.* **1976**, *24*, 71–85.
- (52) Hoult, D. I.; Lauterbur, P. C. *J. Magn. Reson.* **1979**, *34*, 425–433.
- (53) Hoult, D. I. Sensitivity of the NMR Experiment. In *eMagRes*; John Wiley & Sons, Ltd, 2007.

- (54) Hoult, D. I. *Enc. Magn. Reson.* **2007**, DOI: 10.1002/9780470034590.emrstm0491.
- (55) Hoult, D. I.; Richards, R. E. *J. Magn. Reson.* **1976**, *24*, 71–85.
- (56) Minard, K. R.; Wind, R. A. *Concepts Magn. Reson.* **2001**, *13*, 190–210.
- (57) Danieli, E.; Perlo, J.; Blümich, B.; Casanova, F. *Phys. Rev. Lett.* **2013**, *110*, 180801–1–5.
- (58) Siefert, M.; Liebisch, A.; Blumich, B.; Appelt, S. *Nat. Phys.* **2015**, *11*, 767–771.
- (59) Coffey, A. M.; Truong, M.; Chekmenev, E. Y. *J. Magn. Reson.* **2013**, *237*, 169–174.
- (60) Theis, T.; Ortiz, G. X.; Logan, A. W. J.; Claytor, K. E.; Feng, Y.; Huhn, W. P.; Blum, V.; Malcolmson, S. J.; Chekmenev, E. Y.; Wang, Q.; Warren, W. S. *Sci. Adv.* **2016**, *2*, e1501438–e1501438.
- (61) Nelson, S. J.; Kurhanewicz, J.; Vigneron, D. B.; Larson, P. E.; Harzstark, A. L.; Ferrone, M.; van Criekinge, M.; Chang, J. W.; Bok, R.; Park, I.; Reed, G.; Carvajal, L.; Small, E. J.; Munster, P.; Weinberg, V. K.; Ardenkjaer-Larsen, J. H.; Chen, A. P.; Hurd, R. E.; Odegardstuen, L. I.; Robb, F. J.; Tropp, J.; Murray, J. A. *Sci. Transl. Med.* **2013**, *5*, 198ra108.
- (62) Sriram, R.; Van Criekinge, M.; Hansen, A.; Wang, Z. J.; Vigneron, D. B.; Wilson, D. M.; Keshari, K. R.; Kurhanewicz, J. *NMR Biomed.* **2015**, *28*, 1141–1149.
- (63) Keshari, K. R.; Sriram, R.; Van Criekinge, M.; Wilson, D. M.; Wang, Z. J.; Vigneron, D. B.; Peehl, D. M.; Kurhanewicz, J. *Prostate* **2013**, *73*, 1171–1181.
- (64) Rodrigues, T. B.; Serrao, E. M.; Kennedy, B. W. C.; Hu, D.-E.; Kettunen, M. I.; Brindle, K. M. *Nat. Med.* **2013**, *20*, 93–97.
- (65) Reile, I.; Eshuis, N.; Hermkens, N. K. J.; van Weerdenburg, B. J. A.; Feiters, M. C.; Rutjes, F. P. J. T.; Tessari, M. *Analyst* **2016**, *141*, 4001–4005.